

Interrupted coarsening of anisotropic step meander

G. Danker,¹ O. Pierre-Louis,² K. Kassner,¹ and C. Misbah²

¹*Institut für Theoretische Physik, Otto-von-Guericke-Universität Magdeburg, Postfach 4120, D-39016 Magdeburg, Germany*

²*Groupe de Recherche sur les Phénomènes hors Équilibre, LSP CNRS, UMR5588, Université J. Fourier, Grenoble 1, Boîte Postale 87, F38402 Saint Martin d'Hères, France*

(Received 12 January 2003; published 11 August 2003)

We report on the effect of anisotropy on the step meandering instability on vicinal surfaces during molecular beam epitaxy growth. A scenario of interrupted coarsening is found: the lateral length scale of the structure first significantly increases with time and then freezes at a larger length scale. The wavelength selection mechanism results from a nontrivial nonlinear effect of anisotropy. Anisotropy also leads to solutions which drift sideways, resulting from the loss of the back-front symmetry of the meander and the nonvariational character of dynamics.

DOI: 10.1103/PhysRevE.68.020601

PACS number(s): 81.10.Aj, 81.15.Hi, 68.35.Ct

Due to its technological importance in the fabrication of controlled architectures, and as a fundamental problem in the science of nonlinear and irreversible processes, molecular beam epitaxy (MBE) has emerged as a paradigm for the study of out-of-equilibrium driven surfaces. One of the central questions is to build an effective continuum description from the knowledge of basic elementary physical processes.

While continuum descriptions regarding growth on a high symmetry (singular) surface are phenomenological, studies on vicinal surfaces in the step flow regime have now started to reach a mature level of description from microscopic considerations [1–4]. The first stage in studying vicinal surfaces is to determine their step dynamics, from which the dynamics of the full surface can be obtained. Vicinal surfaces are known to suffer two types of instabilities: step bunching and meandering. So far, meandering dynamics can be put into three important classes: (i) spatiotemporal chaos [1] in the presence of atom desorption; (ii) a singular behavior with a meander amplitude growing with time as \sqrt{t} in the absence of desorption, whereas the wavelength is frozen at the early stage; and (iii) a perpetual coarsening [5] if the elastic step-step interaction is relevant. A major task is to answer whether this classification is complete or rather are surface dynamics to reveal new dynamical classes.

We report on a different type of dynamics induced by crystalline anisotropy. We find, under various conditions, the following scenario. In contrast to the isotropic case, anisotropy leads to an initial increase of the wavelength (coarsening), until the wavelength has reached a certain value (which can attain several times that of the linearly unstable mode), beyond which coarsening is interrupted. This scenario plays an important role in the process by which the pattern wavelength is selected. We also discuss the possibility of solutions drifting along the steps. The drift is induced by the lack of front-back symmetry of the step meander along with the nonvariational character of dynamics. Our study is based on a continuum derivation of the steps of nonlinear evolution equations starting from microscopic considerations.

The surface is described by an ensemble of steps separated by terraces. Concentration c of adatoms on each terrace obeys the following quasistatic equation:

$$D \nabla^2 c + F = 0, \quad (1)$$

where D is the adatoms diffusion constant and F the incoming flux. We disregard desorption, and this is legitimate for most practical purposes.

To keep the analysis simple enough, we assume a strong Ehrlich-Schwobel effect (there is no mass exchange between layers) and an instantaneous attachment of adatoms to the steps from the lower side. Then, the concentration fields are subject to the following boundary conditions on both sides of the steps:

$$c|_{+} = c_{\text{eq}}^0 (1 + \Gamma \kappa), \quad D \hat{\mathbf{n}} \cdot \nabla c|_{-} = 0, \quad (2)$$

where $\hat{\mathbf{n}}$ is the normal to the step. Here, c_{eq}^0 is the equilibrium concentration in front of a straight step. $\Gamma = \Omega \tilde{\gamma} / k_B T$, where $\tilde{\gamma}$ is the step stiffness and κ the local step curvature. The $+$ and $-$ signs refer to the ascending and the descending step, respectively. Finally, mass conservation at the step entails the following form for the normal step velocity v_n :

$$v_n = \Omega D \hat{\mathbf{n}} \cdot \nabla c|_{+} + a \partial_s [D_L \partial_s (\Gamma \kappa)]. \quad (3)$$

Ω is the atomic area, a the lattice constant, s the step arc length, and D_L is the macroscopic diffusion constant of atoms along the step.

Anisotropy enters in general in the static and transport coefficients (e.g., D , Γ , and D_L). Let us first consider the case where $\Gamma(\theta) = \Gamma_0 A_\Gamma(\theta)$ and $D_L(\theta) = D_{L0} A_L(\theta)$. For definiteness, we adopt a fourfold symmetry (any other symmetry can be dealt with along the same lines):

$$A_{\Gamma,L}(\theta) = 1 + \epsilon_{\Gamma,L} \cos[4(\theta - \theta_{\Gamma,L})]. \quad (4)$$

Here, $\theta = \arctan(\partial_x \zeta)$ is the angle of the local step's normal with respect to its average [$\zeta(x, t)$ refers to the instantaneous step position], $\epsilon_{\Gamma,L} \in [0, 1[$ measures the strength of the anisotropy, and $\theta_{\Gamma,L}$ denotes the angle along which Γ or D_L has its largest value.

Our starting point is to perform the linear stability analysis of a uniform train with straight steps (separated by the same distance ℓ) moving altogether at constant speed $\Omega F \ell$.

Steps are morphologically unstable against fluctuations with wavelengths larger than a certain critical wavelength λ_c [6]. The most unstable mode is found to be in-phase meandering with wavelength

$$\lambda_m = 4\pi \left(\frac{\Gamma(0)[D_S \ell + D_L(0)a]}{\Omega F \ell^2} \right)^{1/2}, \quad (5)$$

where $D_S = D\Omega c_{\text{eq}}^0$ and we have $\lambda_c = \lambda_m / \sqrt{2}$. We shall thus restrict our attention to the in-phase mode, where all steps have the same meander $\zeta(x, t)$. The model equations (1)–(4) are expanded in terms of a small parameter $\xi = (2\pi\ell/\lambda_m)^2$. The linear stability analysis dictates the relevant scales $x \sim \xi^{-1/2}$ and $t \sim \xi^{-2}$. As in Refs. [3,4], the scaling of the meander is singular $\zeta \sim \xi^{-1/2}$. Following Ref. [4], the multiscale expansion of the model equations (1)–(3) then provides a highly nonlinear evolution equation for $\zeta(x, t)$:

$$\partial_t \zeta = -\partial_x \left[\sigma_0 \frac{\partial_x \zeta}{1 + (\partial_x \zeta)^2} - \mathcal{M}_0 \partial_x (\Gamma \kappa) \right], \quad (6)$$

$$\mathcal{M}_0 = D_S \ell (1 + (\partial_x \zeta)^2)^{-1} + D_L a [1 + (\partial_x \zeta)^2]^{-1/2}, \quad (7)$$

where $\sigma_0 = \Omega F \ell^2 / 2$. This equation takes the form of a conservation law $\partial_t \zeta + \partial_x J = 0$, where J can be regarded as a mass current along the step. Equation (6) assumes a similar form as in the isotropic case [3]. However, we show here that anisotropy drastically affects dynamics.

In the idealized isotropic model [3,4], the meandering wavelength λ_m is found to be selected at the early stage of the instability; it is not affected by the nonlinear dynamics. However, the amplitude grows indefinitely as \sqrt{t} . We shall refer to this solution as *diverging* solutions. In Ref. [3], such a behavior has been traced back to the absence of steady states solutions for Eq. (6) with a wavelength $\lambda \gg \lambda_c$. In contrast, it is found that anisotropy allows for a continuous family of solutions with $\lambda > \lambda_c$.

We first turn our attention to the situation where Eq. (6) attains the $(x) \rightarrow (-x)$ symmetry. This happens for $\theta_{\Gamma, L} = 0$ or $\pi/4$. For symmetry reasons, a vanishing lateral drift and mass current J along the step are then expected for steady solutions. These solutions are parametrized by $m_0 = \max(m)$, where $m = \partial_x \zeta / [1 + (\partial_x \zeta)^2]^{1/2} = \sin \theta$. Using an analogy to point mechanics in a one-dimensional potential [4], the wavelength λ_0 of stationary solutions is found to be

$$\lambda = \frac{\lambda_m}{2\pi} \int_{-m_0}^{m_0} \frac{A_\Gamma(m)}{[V(m_0) - V(m)]^{1/2}} dm, \quad (8)$$

where

$$V(m) = \int_{m_0}^m \frac{A_\Gamma(m') m' dm'}{\sqrt{1 - m'^2} \tilde{\beta} + (1 - \tilde{\beta}) A_L(m')} \quad (9)$$

and $\tilde{\beta} = D_S l / (D_S l + D_L a)$. Consider first an anisotropic line tension and $D_L = 0$. When $\theta_\Gamma = 0$, the analysis of the above equations reveals that the steady-state solutions possess a wavelength which decreases upon increasing the anisotropy

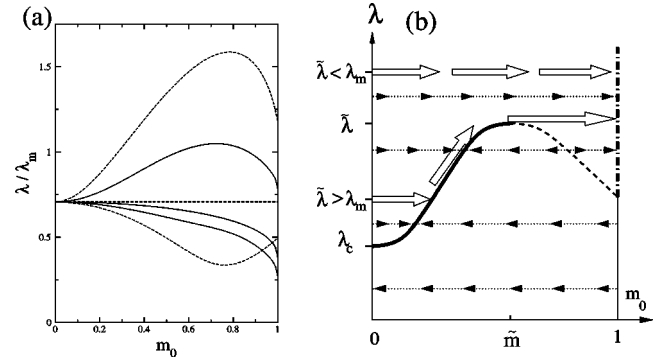


FIG. 1. (a) λ as a function of m_0 . Solid curves: no step edge diffusion ($D_L = 0$). Dashed curves: no detachment from steps ($c_{\text{eq}}^0 = 0$) with isotropic Γ and anisotropic D_L . In both cases, from lower to upper curve: $\epsilon_{\Gamma, L} = 0.7$ with $\theta_{\Gamma, L} = 0$, $\epsilon_{\Gamma, L} = 0$, and $\epsilon_{\Gamma, L} = 0.7$ with $\theta_{\Gamma, L} = \pi/4$. (b) The stable (solid line) and unstable (dashed line) branches are shown. Small black arrows indicate the flow of the highest slope for one cell in a box with periodic boundary conditions. White arrows show the path of the average wavelength in an extended system.

strength, as shown in Fig. 1. Therefore, as in the isotropic case, steady-state solutions do not exist for $\lambda > \lambda_c$.

However, if $\theta_\Gamma = \pi/4$, we discover a qualitative change of the overall picture of steady-state solutions. More precisely, the quantity $d^2\lambda/dm_0^2$ evaluated at $m_0 = 0$ becomes positive for $\epsilon_\Gamma > 0.068$. This is a signature of a transition from a subcritical to a supercritical bifurcation (this defines the dynamical analog of the so-called Lifshitz point in phase transition phenomena). Due to the supercritical nature of the bifurcation, steady-state solutions should be stable with respect to amplitude fluctuations around $m_0 = 0$. This stability was checked numerically by direct integration of the evolution equation, Eq. (6), with one cell in a periodic box of size L_b . The branch of steady states is stable up to the maximum at $\tilde{m}, \tilde{\lambda}$. Close to the maximum the bifurcation is of saddle-node nature, implying that the decreasing part of the branch at $m_0 > \tilde{m}$ is unstable. Beyond the maximum, we find “diverging” solutions whose amplitudes increase indefinitely $\sim t^{1/2}$ at large slopes $m_0 \rightarrow 1$. It is worthwhile to mention here that the wavelength of these latter asymptotic solutions can be arbitrarily large [7] [$\lambda > \lambda(m_0 = 1)$]. This is solely determined by initial conditions.

Consider now a situation where the box size is large enough $L_b > \lambda_m, \tilde{\lambda}$. Starting from small initial perturbations, we expect the step to exhibit first the linear fastest growing mode with wavelength λ_m . As shown in Fig. 1, two situations may then be encountered. If anisotropy is weak, $\epsilon_\Gamma < \epsilon_\Gamma^c = 0.668 \dots$, one has $\tilde{\lambda} < \lambda_m$. The meander amplitude increases without bound. The wavelength is frozen and the amplitude grows asymptotically as $t^{1/2}$. On further increase of the anisotropy strength, and beyond a critical value $\epsilon_\Gamma > \epsilon_\Gamma^c$, one has $\lambda_m < \tilde{\lambda}$. The meander amplitude first increases in the course of time until it reaches a steady state at λ_m . Then, the average wavelength of the cells increases via cell coalescence. The process of coarsening is interrupted when the average wavelength reaches $\tilde{\lambda}$ (actually for a finite box

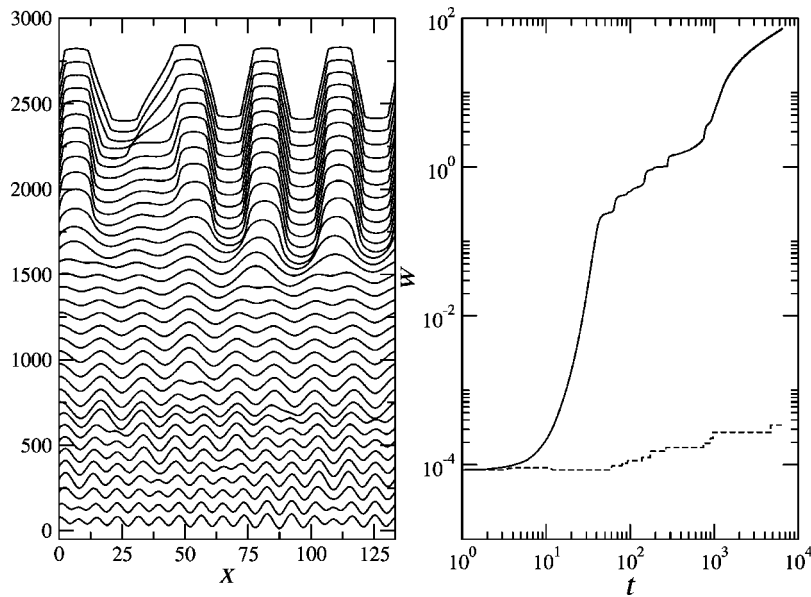


FIG. 2. A snapshot of the meander $\zeta(x,t)$. We show the case where steps are stabilized by anisotropic line diffusion, i.e., $c_{eq}=0$, with $\epsilon_L=0.92$ and $\theta_L=\pi/4$ ($\tilde{\lambda}=3.1\lambda_m>\lambda_m$). The left panel shows the meander at different times (amplitude rescaled for better visibility). The right panel shows the amplitude (solid line) and the average wavelength (dashed) as a function of time (arbitrary units).

the chosen wavelength is slightly larger). Once this stage is reached, the amplitude of each cell grows as $\sim t^{1/2}$, while coarsening should stop. We expect thus the final wavelength of the cells to be $\max(\lambda_m, \tilde{\lambda})$.

As shown in Fig. 1(a), it is noteworthy that the same picture holds when allowance is made for line diffusion anisotropy [9], even if line tension is isotropic.

Simulations of Eq. (6) support this picture. In Fig. 2, we show the meander evolution for a system having an extent $L_b=15\lambda_m$. The early emerging stage (with noisy initial conditions) exhibit 16 cells. Later, a coarsening process takes place, leading to the final expected number of $\text{int}(L_b/\tilde{\lambda})=4$ cells.

For $\epsilon_{\Gamma,L}\rightarrow 1$, the following asymptotic behavior is extracted from Eq. (8):

$$\tilde{\lambda}_{\Gamma,L} = \alpha \frac{\lambda_m}{(1 - \epsilon_{\Gamma,L})^{1/2}}. \quad (10)$$

$\tilde{\lambda}_{\Gamma,L}$ does not depend on the precise form of anisotropy (4), which only enters the prefactor α . Using Eq. (4), we find $\alpha_{\Gamma}=0.564$ when $D_L=0$.

Hitherto, we have considered only the situation with $\theta_{L,\Gamma}=0,\pi/4$. Since interrupted coarsening occurs for $\theta_{L,\Gamma}=\pi/4$ and not for $\theta_{L,\Gamma}=0$, we suspect the existence of a critical angle $\theta^*(\epsilon)\in[0,\pi/4]$, beyond which interrupted coarsening is revealed. We have determined $\theta^*(\epsilon)$ numerically. The results are plotted in Fig. 3.

Another important question concerns the possibility that the pattern may drift sideways due to the lack of the $x\rightarrow -x$ symmetry of Eq. (6), a fact that occurs when $\theta_{L,\Gamma}\neq 0,\pi/4$. The numerical solution of Eq. (6) reveals no drift. This is *a priori* surprising inasmuch as the evolution equation is not symmetric. A close inspection of Eq. (6) reveals that in the evolution equation for $u=\partial_x\zeta$, the $(x)\rightarrow(-x)$ symmetry is reinstated. This is a consequence of the fact that Eq. (6) still possesses the simultaneous symmetry group

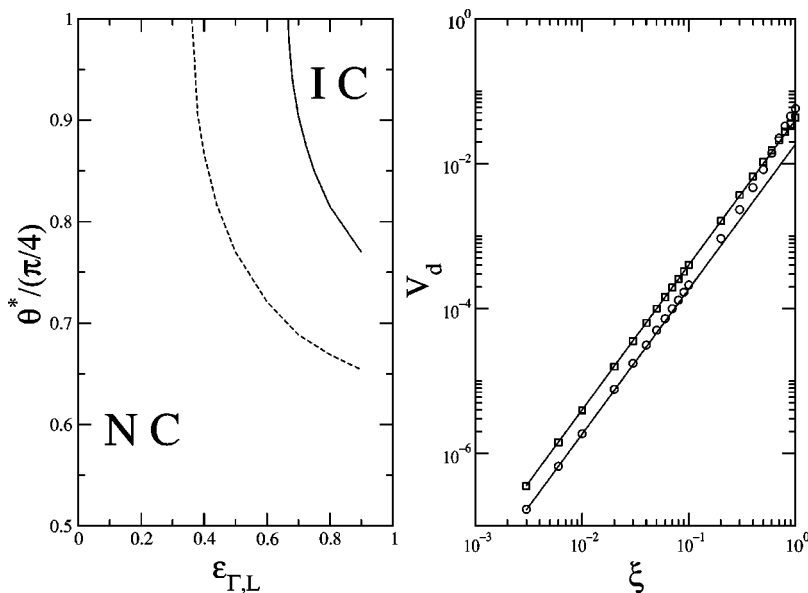


FIG. 3. The critical angle θ^* as a function of ϵ . Solid lines are for Γ and dashed lines for D_L anisotropy. IC and NC indicate the regions with interrupted coarsening and with no coarsening, respectively. Right panel: V_d as a function of the small parameter ξ . The solid lines are $\sim \xi^2$.

$(x, \zeta) \rightarrow (-x, -\zeta)$. Thus, the drift dilemma is resolved since the symmetric solution should not naturally drift.

Drift occurs however when higher-order nonlinear contributions are considered. Indeed, they destroy the above-mentioned symmetry group. At higher order, the evolution equation still has the same form as Eq. (6), albeit σ_0 and \mathcal{M}_0 must be substituted by $\sigma = \sigma_0 \{1 - \kappa \ell [\cos(\theta)^{-1} + 2 \cos(\theta)]/3\}$ and $\mathcal{M} = \mathcal{M}_0 + \kappa \ell^2 D_S \cos(\theta)/2$. The numerical solution of this equation does indeed present drifting steady states. An expansion at small ξ allows one to extract the functional dependence of the drift velocity:

$$V_d = \frac{\beta}{2^{3/2}} \frac{(\Omega F)^2 \ell^5}{\Gamma(0)[D_S \ell + D_L(0)a]}, \quad (11)$$

where β depends on the anisotropy functions A_Γ , A_L , and on λ . We have $\beta=0$ for $m_0=0$ (i.e., $\lambda=\lambda_c$) and for $m_0=1$ (solutions with vertical slopes). As shown in Fig. 3, Eq. (11) was checked for small ξ . Two remarks are in order. First, the interrupted coarsening scenario is qualitatively preserved in the presence of a drift. Second, in the pure terrace diffusion regime ($D_L=0$), not only does V_d vanish, but so does J . This stems from the (accidental) variational character of the evolution equation (6). Indeed, Eq. (6) can be written as $\partial_t \zeta = \partial_x [M \partial_x (\delta \mathcal{F} / \delta \zeta)]$, with

$$\mathcal{F} = \int dx \left[\frac{\nu}{2} \zeta^2 + \gamma (1 + (\partial_x \zeta)^2)^{1/2} \right], \quad (12)$$

where $\nu = k_B T (F \ell / 2 D_S)$ and $M = (\Omega / k_B T) D_S \ell (1 + (\partial_x \zeta)^2)^{-1}$. \mathcal{F} is a Lyapunov functional, which always decreases with time:

$$\frac{d}{dt} \mathcal{F} = \int dx \partial_t \zeta \frac{\delta \mathcal{F}}{\delta \zeta} = - \int dx M \left[\partial_x \left(\frac{\delta \mathcal{F}}{\delta \zeta} \right) \right]^2 \leq 0. \quad (13)$$

For a drifting steady state, the meander $\zeta(x, t)$ only depends on the variable $x' = x - V_d t$. The change of variable $x \rightarrow x'$ in Eq. (12) then shows that \mathcal{F} is time independent (i.e., $d\mathcal{F}/dt = 0$). Since $M \geq 0$, one has either $\partial_x (\delta \mathcal{F} / \delta \zeta) = 0$ or $M = 0$,

from Eq. (13). Therefore, $J = M \partial_x (\delta \mathcal{F} / \delta \zeta) = 0$, and from $V_d \partial_x \zeta = \partial_x J$ one also concludes that $V_d = 0$. Since subdominant terms break the variational character of Eq. (6), they restore nonvanishing J and V_d , as confirmed by the numerical solution of Eq. (6) with subdominant terms.

In MBE experiments at moderate temperature, anisotropy is usually strong. Consider, for example, a square lattice with nearest neighbor interactions. In the case of Cu(100) surface at room temperature [10], we find $\eta_\Gamma = \Gamma(10)/\Gamma(11) \sim 86$ [11]. Although the angular dependence in real systems may be different from Eq. (4) [12], a qualitative comparison is obtained by using the ratio of the largest on the smallest value of the stiffness needed to observe interrupted coarsening with Eq. (4): $\eta_\Gamma^c = (1 + \epsilon_\Gamma^c)/(1 - \epsilon_\Gamma^c) \approx 5 < \eta_\Gamma$. Furthermore, Liu and Evans [13] have shown from kinetic Monte Carlo simulations, that, in the presence of a kink rounding barrier, $\eta_L = D_L(10)/D_L(11) \sim 10 > \eta_\Gamma^c \approx 2.13$ (calculated for isotropic Γ). Therefore, both line stiffness and line diffusion anisotropies should induce observable [14] interrupted coarsening for (11) steps [but probably not for (10) steps].

In summary, interrupted coarsening occurs as a subtle compromise between, on the one hand, the basic diffusive instability that tends to drive the meander towards an indefinitely growing amplitude and, on the other hand, the anisotropy effect which acts as a pinning force—of thermodynamic or kinetic origin—along preferred crystalline orientations. Surprisingly enough, the step temporal evolution seems to be linked with the structure of the steady-state branch (as in Fig. 1) [15].

Additional effects, such as a finite anisotropic Schwoebel effect, may be added to the model. Interrupted or endless coarsening are also obtained [9], depending on the shape of the steady-state branch. In a previous work [5], it was shown that step interactions induce endless coarsening. Since it leads to an infinite steady-state branch, the elastic interaction restores infinite coarsening in the presence of anisotropy [9].

This work was supported by the German-French cooperation program PROCOPE, Grant Nos. D/0122928 and 04643YK. Moreover, financial support from the Deutsche Forschungsgemeinschaft under Grant No. Em 68/3-1 is acknowledged.

-
- [1] I. Bena, C. Misbah, and A. Valance, Phys. Rev. B **47**, 7408 (1993); O. Pierre-Louis and C. Misbah, Phys. Rev. Lett. **76**, 4761 (1996).
 [2] M. Sato, M. Uwaha, and Y. Saito, Europhys. Lett. **32**, 639 (1995); C. Misbah and O. Pierre-Louis, Phys. Rev. E **53**, R4318 (1996); M. Sato and M. Uwaha, J. Cryst. Growth **198-199**, 38 (1999).
 [3] O. Pierre-Louis, C. Misbah, Y. Saito, J. Krug, and P. Politi, Phys. Rev. Lett. **80**, 4221 (1998).
 [4] F. Gillet, O. Pierre-Louis, and C. Misbah, Eur. Phys. J. B **20**, 519 (2000).
 [5] S. Paulin, F. Gillet, O. Pierre-Louis, and C. Misbah, Phys. Rev. Lett. **86**, 5538 (2001).
 [6] G.S. Bales and A. Zangwill, Phys. Rev. B **41**, 5500 (1990).
 [7] Initial conditions determine the wavelength of each cell, which

- can be arbitrarily wide. This contradicts the results of Ref. [8].
 [8] J. Kallunki and J. Krug, Phys. Rev. E **62**, 6229 (2000).
 [9] G. Danker, O. Pierre-Louis, K. Kassner, and C. Misbah (unpublished).
 [10] M. Giesen, Prog. Surf. Sci. **68**, 1 (2001).
 [11] On Cu(100) surfaces, which have an fcc structure, (10) corresponds to [110] and (11) to [100].
 [12] C. Rottman and M. Wortis, Phys. Rev. B **24**, 6274 (1981); S. Dieluweit, H. Ibach, M. Giesen, and T. L. Einstein (unpublished).
 [13] D.-J. Liu and J.W. Evans, Phys. Rev. B **66**, 165407 (2002).
 [14] T. Maroutian, L. Douillard, and H.-J. Ernst, Phys. Rev. Lett. **83**, 4353 (1999); Phys. Rev. B **64**, 165401 (2001).
 [15] P. Politi and C. Misbah (unpublished).